NeuroImage: Clinical 22 (2019) 101780

Contents lists available at ScienceDirect

NeuroImage: Clinical

journal homepage: www.elsevier.com/locate/ynicl

Altered grey matter volume, perfusion and white matter integrity in very low birthweight adults

Maddie J. Pascoe[a,*], Tracy R. Melzer[a,b], L. John Horwood[c], Lianne J. Woodward[d], Brian A. Darlow[e]

[a] New Zealand Brain Research Institute, Christchurch 8011, New Zealand
[b] Department of Medicine, University of Otago, Christchurch 8011, New Zealand
[c] Department of Psychological Medicine, University of Otago, Christchurch 8011, New Zealand
[d] School of Health Sciences, University of Canterbury, Christchurch 8041, New Zealand
[e] Department of Paediatrics, University of Otago, Christchurch 8011, New Zealand

ARTICLE INFO

Keywords:
Magnetic resonance imaging (MRI)
Very low birth weight
Preterm
Brain
Adult
Cerebral perfusion

ABSTRACT

This study examined the long-term effects of being born very-low-birth-weight (VLBW, < 1500 g) on adult cerebral structural development using a multi-method neuroimaging approach. The New Zealand VLBW study cohort comprised 413 individuals born VLBW in 1986. Of the 338 who survived to discharge, 229 were assessed at age 27–29 years. Of these, 150 had a 3 T MRI scan alongside 50 healthy term-born controls. The VLBW group included 53/57 participants born < 28 weeks gestation. MRI analyses included: a) structural MRI to assess grey matter (GM) volume and cortical thickness; b) arterial spin labelling (ASL) to quantify GM perfusion; and c) diffusion tensor imaging (DTI) to measure white matter (WM) integrity. Compared to controls, VLBW adults had smaller GM volumes within frontal, temporal, parietal and occipital cortices, bilateral cingulate gyri and left caudate, as well as greater GM volumes in frontal, temporal and occipital areas. Thinner cortex was observed within frontal, temporal and parietal cortices. VLBW adults also had less GM perfusion within limited temporal areas, bilateral hippocampi and thalami. Finally, lower fractional anisotropy (FA) and axial diffusivity (AD) within principal WM tracts was observed in VLBW subjects. Within the VLBW group, birthweight was positively correlated with GM volume and perfusion in cortical and subcortical regions, as well as FA and AD across numerous principal WM tracts. Between group differences within temporal cortices were evident across all imaging modalities, suggesting that the temporal lobe may be particularly susceptible to disruption in development following preterm birth. Overall, findings reveal enduring and pervasive effects of preterm birth on brain structural development, with individuals born at lower birthweights having greater long-term neuropathology.

1. Introduction

The late second and third trimester of pregnancy is a critical period of brain development during which the brain undergoes a five-fold increase in cortical surface area (Kapellou et al., 2006; Moeskops et al., 2015). At the microstructural level, neurons begin to differentiate functionally and to form connections with each other (Huttenlocher and Dabholkar, 1997). Myelination of these new networks also begins from around 32 weeks to improve neural conduction (Keunen et al., 2017). For the infant born very preterm (< 32 weeks gestation) and/or very low birth weight (< 1500 g birth weight), these important developmental events occur at a time when the infant is acutely unwell and being cared for in the ex-utero environment of the Neonatal Intensive Care Unit (NICU). Given their physiological and neurological immaturity, infants born very preterm are at high risk of cerebral white matter (WM) injury and altered grey matter development (Back, 2017; Kinney and Volpe, 2018). Negative environmental exposures such as stress, pain and under-nutrition, may also adversely affect the developing brain (Belfort and Ehrenkranz, 2017; Brummelte et al., 2012; Grunau et al., 2006). As a result, these infants are at high risk for a range of neurobehavioral problems (Anderson et al., 2015; Woodward et al., 2006).

Advanced MRI scanning techniques have been important in advancing our understanding of the effects of being born very preterm (VP) and/or very low birth weight (VLBW) on brain structure and function. These studies have extended from infancy through to

* Corresponding author at: New Zealand Brain Research Institute, 66 Stewart Street, Christchurch 8011, New Zealand.
E-mail addresses: maddie.pascoe@nzbri.org (M.J. Pascoe), tracy.melzer@otago.ac.nz (T.R. Melzer), john.horwood@otago.ac.nz (L.J. Horwood), lianne.woodward@canterbury.ac.nz (L.J. Woodward), brian.darlow@otago.ac.nz (B.A. Darlow).

https://doi.org/10.1016/j.nicl.2019.101780
Received 22 November 2018; Received in revised form 11 March 2019; Accepted 14 March 2019
Available online 15 March 2019

childhood and adolescence (see for reviews: (de Kieviet et al., 2012; Li et al., 2015; Raju et al., 2017), and even more recently, into young adulthood (Nosarti et al., 2014; Raju et al., 2017; Rimol et al., 2019). Volumetric data have consistently demonstrated that children and adolescents born VLBW are characterized by smaller total brain volumes than their same age peers born full term (37–41 weeks gestation) (Kesler et al., 2004; Nosarti et al., 2002). Regionally-specific reductions, above and beyond global loss, have also been observed within the temporal lobe (Kesler et al., 2004), basal ganglia, amygdala and hippocampus (Peterson et al., 2000) of preterm/VLBW children. During adolescence, smaller absolute GM volume has been found within frontal, temporal and occipital cortices, thalami, putamen and caudate nuclei (Nosarti et al., 2008). Smaller relative GM volumes have also been reported in frontal and temporal cortices, as well as the parietal lobe, cingulate gyrus, thalami and parahippocampus (Lean et al., 2017). A somewhat consistent picture is emerging from studies of adults born VP or VLBW, with evidence of smaller relative GM volumes in frontal, temporal and occipital cortices as well as the cingulate gyrus (Nosarti et al., 2014), thalamus, caudate nuclei (Bjuland et al., 2014; Nosarti et al., 2014) and globus pallidus (Bjuland et al., 2014). Relatedly in VLBW young adults, thinner cortex has also been reported within frontal (Bjuland et al., 2013), parietal and temporal cortices (Bjuland et al., 2013; Martinussen et al., 2005; Nagy et al., 2010; Rimol et al., 2019), and thicker cortex within temporal (Martinussen et al., 2005; Nagy et al., 2010), frontal and occipital regions (Bjuland et al., 2013; Martinussen et al., 2005; Nagy et al., 2010; Rimol et al., 2019).

DTI studies also reveal microstructural alterations in cerebral WM of individuals born VLBW, with these differences observable throughout childhood and adolescence (Nagy et al., 2003; Skranes et al., 2007). For example, Constable et al. (2008) found fractional anisotropy (FA) to be lower within uncinate, inferior and superior frontooccipital fasciculi, splenium of the corpus callosum and external capsules in 12 year-olds born very preterm as compared to controls. Furthermore, a study from Norway found lower FA within numerous WM tracts in former VLBW individuals when assessed at ages15-years and 18–22 years (Eikenes et al., 2011; Skranes et al., 2007). At age 26, reduced FA in frontal lobe pathways was also found in the Norwegian cohort (Rimol et al., 2019).

Taken together, these studies suggest that alterations in brain structure and function associated with VP/VLBW persist from infancy through to late adolescence/early adulthood. However, studies beyond early adulthood are limited, with most studies employing a single method approach. Further, to our knowledge, GM perfusion has not been examined in this population beyond infancy despite preliminary data showing that preterm birth may be associated with both increased and decreased cerebral perfusion (Mahdi et al., 2018). Perfusion dysfunction may be associated with structural alterations, and has even been shown to precede structural loss in some scenarios (Chételat et al., 2007; Gonzalez-Redondo et al., 2014). The mechanisms underlying disrupted perfusion associated with very preterm birth are complex, but may reflect alteration of cardiovascular autonomic control, immature hemodynamics (which may in turn increase the risk of haemorrhage or hypoxic-ischemic injury), or increased physiologic stress (Brew et al., 2014; Fyfe et al., 2014). Thus, we suggest that cerebral perfusion MRI may also provide valuable insight into the neurological impacts of being born very preterm/VLBW, in early adulthood. Finally, relationships between structural brain outcomes and birthweight have been reported in children and adolescents born preterm/VLBW (Allin et al., 2011; Bjuland et al., 2013; Eikenes et al., 2011; Kesler et al., 2004) which suggest that those born at lower gestational ages and birth weights tend to have higher risks of brain structural and functional alterations. Thus, we also examined the extent to which the degree of prematurity continued to have an influence on later structural brain outcomes during adulthood in this unique national cohort.

Against this background, the current study aimed to use a multimethod approach to examine differences in GM volume, cortical thickness, perfusion and WM integrity in a national cohort of adults born with VLBW in New Zealand during 1986. Additionally, associations between weight at birth and later brain outcomes were examined. We hypothesized that the VLBW group would exhibit lower GM volumes and perfusion, thinner cortex and poorer WM integrity, compared to term-born controls. We also hypothesized that in VLBW adults, birthweight would be positively associated with measures of brain structural neuropathology.

2. Methods

2.1. Standard protocol approvals, registrations, and patient consents

The study was approved by the Upper South B Regional Ethics Committee of New Zealand. Written informed consent was obtained from all participants in the study.

2.2. Participants

The protocol and methods for the New Zealand VLBW Follow-up Study have been described previously (Darlow et al., 2015). Briefly, a total of 229 members of a national cohort of 323 VLBW survivors born in 1986 (71% retention) underwent a comprehensive 2-day health and neuropsychological assessment in one centre at age 27–29 years. Twenty-one of the remaining 94 cohort members answered a comprehensive questionnaire, 38 declined to participate and 35 were untraced. A control group of 100 subjects born healthy at term in 1986 were first recruited at age 23–24 through either a process of peer nomination by a cohort member or via random sampling from national electoral rolls, balancing for gender, ethnicity and regional distribution (Darlow et al., 2015).

Funding was available for 200 advanced cranial MRI scans. We planned to scan all VLBW adults born at < 28 weeks ($n = 57$) given the known higher neurodevelopmental risks and limited number of studies examining this group. However, three of these subjects were unable to be scanned due to the presence of a cerebral shunt, a pregnancy, and difficulties with claustrophobia. A further scan was not readable. In addition to this high risk group, a random sample of the remaining VLBW cohort were scanned, bringing the total number of VLBW participants having readable scans to 150. Of the VLBW participants having an MRI, 4% had moderate/severe neurosensory disability at age 7–8 years, compared with 14% of those not scanned, with more of the latter being unable or unwilling to take part in the full study. The control group consisted of the first 50 controls sequentially who agreed to an MRI. A profile of the social background, medical and neurodevelopmental characteristics of the two study groups is provided in Table 1.

2.3. MRI acquisition

Imaging was conducted on a 3 T General Electric HDxt scanner (GE Healthcare, Waukesha, USA) with an eight-channel head coil.

2.3.1. Conventional structural

Volumetric T1-weighted (inversion-prepared spoiled gradient recalled echo (SPGR), TE/TR = 2.8/6.6 ms, TI = 400 ms, flip angle = 15 deg., acquisition matrix = 256 × 256 × 170, FOV = 250 mm, slice thickness = 1 mm, voxel = 0.98 × 0.98 × 1.0 mm^3) and clinical T2 and T2 FLAIR (TE/TR = 116/9000 ms, TI = 2250 ms, flip angle = 90 deg., acquisition matrix = 320 × 320 × 32, reconstruction matrix = 512 × 512 × 32, FOV = 220 mm, slice thickness = 3 mm, gap = 1.5 mm, reconstructed voxel = 0.43 × 0.43 × 4.5 mm^3) images were collected.

2.3.2. Pseudo-continuous arterial spin labelling (PCASL)

A stack of spiral, fast spin echo acquired images were prepared with pseudo-continuous arterial spin labelling and background suppression

Table 1
Comparison of demographic and perinatal characteristics of the surviving VLBW cohort who were assessed on MRI with those not assessed and with controls.

Measure	VLBW assessed on MRI (N = 150)	VLBW not assessed on MRI (N = 173)	P[a]	Controls (N = 50)	P[b]
Mean (SD) age at scan	28.5 (1.2)	–	–	27.7 (0.5)	< 0.001
% (n) Male	41.3 (62)	52.0 (90)	0.055	40.0 (20)	0.87
% (n) Māori/Pacific Island ethnicity	28.7 (43)	34.7 (60)	0.25	18.0 (9)	0.14
Mean (SD) birthweight (g)	1077 (238)	1213 (215)	< 0.001		
% (n) < 1000 g	38.0 (57)	15.6 (27)	< 0.001		
Mean (SD) gestation (weeks)	28.8 (2.6)	29.6 (2.3)	0.002		
% (n) < 28 weeks gestation	35.3 (53)	15.6 (27)	< 0.001		
Mean (SD) Apgar 5 min	7.8 (1.9)	8.0 (1.7)	0.51		
% (n) SGA	30.7 (46)	27.2 (47)	0.49		
% (n) Vaginal delivery	43.8 (64)	40.1 (69)	0.5		
% (n) Sepsis	20.7 (31)	26.7 (46)	0.2		
% (n) ANS	54.7 (82)	59.5 (103)	0.38		
% (n) RDS	56.7 (85)	56.1 (97)	0.91		
% (n) BPD	20.7 (31)	21.4 (37)	0.87		
% (n) ROP	25.0 (36)	17.4 (27)	0.11		
% (n) Any neurosensory disability (age 7–8 years)	16.6 (24)	33.1 (50)	0.001		
% (n) Mod/severe disability (age 7–8 years)	4.1 (6)	13.9 (21)	0.004		

SGA: small for gestational age (birthweight < 10% centile), RDS: respiratory distress syndrome, BPD: bronchopulmonary dysplasia (oxygen requirement at 36 weeks post-menstrual age), ANS: antenatal corticosteroids, ROP: retinopathy of prematurity. Moderate or severe disability at 7–8 years of age was defined as cerebral palsy in non-ambulant children or in ambulant children causing considerable limitation of movement; bilateral sensorineural deafness requiring hearing aids; bilateral blindness; or an IQ score of > 2 SD below the test mean (< 70) on the Revised Wechsler Intelligence Scale for Children (WISC-R). Any neurosensory disability at 7–8 years of age also included cerebral palsy with only minor limitation of movement and mild cognitive impairment (IQ 1-2 SD below the mean).

[a] Comparisons of VLBW assessed and not assessed by *t*-test or chi square.

[b] Comparisons of VLBW assessed and Controls by *t*-test or chi square.

to measure whole brain perfusion quantitatively (Dai et al., 2008): TR = 6 s, echo spacing = 9.2 ms, post-labelling delay = 1.525 s, labelling duration = 1.5 s, eight interleaved spiral arms with 512 samples at 62.5 kHz bandwidth and 30 phase encoded 5 mm thick slices, NEX = 5, units: ml/100 g/min. Participants were asked to focus on a fixation cross during the PCASL scan.

2.3.3. Diffusion tensor imaging (DTI)

A 2D diffusion-weighted, spin echo, echo planar imaging sequence was used to measure microstructural integrity, with diffusion weighting in 64 uniformly distributed directions (b = 1000 s/mm^2) and 8 acquisitions without diffusion weighting (b = 0 s/mm^2): TE/TR = 96/10000 ms, flip angle = 90 deg., acquisition matrix = 128 × 128 × 74, FOV = 250 mm, slice thickness = 2 mm, voxel size = 1.95 × 1.95 × 2 mm^3, NEX = 1, ungated.

2.4. MRI preprocessing

2.4.1. Structural preprocessing

CAT12 (r934, http://www.neuro.uni-jena.de/cat/), a toolbox of SPM12 (v6470, http://www.fil.ion.ucl.ac.uk/spm/), running in Matlab 7.10.0 (R2010a), was used to process T1-weighted structural images. Briefly, images were bias corrected, spatially normalized via DARTEL (using the DARTEL template provided within CAT12, registered to MNI space), modulated to compensate for the effect of spatial normalization, and classified into grey matter (GM), white matter (WM), and cerebrospinal fluid (CSF), all within the same generative model (Ashburner and Friston, 2005). The segmentation procedure was extended by accounting for partial volume effects (Tohka et al., 2004), applying adaptive maximum a posteriori estimations (Rajapakse et al., 1997), and using a hidden Markov Random Field model (Cuadra et al., 2005). The resulting modulated, normalized GM partitions were then smoothed using an 8 mm full-width-at-half-maximum (FWHM) Gaussian kernel.

2.4.2. Cortical thickness

Cortical thickness was estimated using the automated FreeSurfer stream (v6.0, http://surfer.nmr.harvard.edu); cortical thickness maps were smoothed with a 10 mm FWHM Gaussian kernel and separately with a 20 mm FWHM Gaussian kernel. Sections 3.2.2 and 3.3.2 report results from analyses using cortical thickness maps smoothed with a 10 mm FWHM Gaussian kernel. Results obtained from 20 mm smoothing are available in the Supplementary material (Figs. S1 and S2).

2.4.3. Pseudo-continuous arterial spin labelled preprocessing

Quantified cerebral perfusion images were co-registered to T1-weighted structural images. Subject-specific ICV masks were created using the 'reverse brain mask method', which has been shown to provide an accurate estimate for ICV (Hansen et al., 2015). This method applies the inverse deformation fields from the structural images (produced during the DARTEL normalization procedure) to the ICV mask supplied in SPM12, which warps the ICV mask from standard space to subject space for each participant. Subject-specific ICV masks were resliced, dilated, and applied to the quantified perfusion image to remove non-brain tissue from the perfusion images. Given the age range of the participants in the study, we deemed the SPM12 ICV mask an appropriate starting point for ICV estimation. Perfusion images underwent further processing with the partial volume correction using modified least trimmed squares (PVC-mLTS) toolbox in SPM5 (Liang et al., 2013). The quantified, co-registered, brain extracted, partial volume corrected perfusion images were then DARTEL normalized using the structural parameters (no modulation) and smoothed with an 8 mm FWHM Gaussian kernel. One participant did not receive ASL and was therefore excluded from analyses of cerebral perfusion. Thus, sample size for perfusion analyses was $n = 199$ ($n_{vlbw} = 149$, $n_{control} = 50$).

2.4.4. Creation of Grey matter mask

A mean GM mask was created from the normalized GM images of 49 controls and 49 randomly selected participants from the VLBW group, in order to restrict perfusion analyses to GM. The mean GM image was thresholded at 0.15; slices below the mid-cerebellum were set to zero to exclude spiral artefact and poor image quality of PCASL scans in this region.

2.4.5. DTI preprocessing

Diffusion-weighted images were pre-processed and analysed using

Table 2
Global MRI metrics in VLBW and full term controls.

Imaging metrics	VLBW Mean (SD)	Control Mean (SD)	t	p
Grey matter (cm^3)	669 (61)	723 (62)	−2.21	0.03
Grey matter proportion	0.445 (0.019)	0.449 (0.016)	−2.32	0.022
White matter (cm^3)	513 (61)	558 (66)	−0.93	0.435
Cerebrospinal fluid (cm^3)	322 (44)	332 (50)	2.48	0.014
Intracranial volume (cm^3)	1504 (140)	1613 (162)	−5.21	< 0.0001
Mean GM perfusion(ml/100 g/min)	50.6 (8.8)	51.6 (7.6)	−0.99	0.33
Partial volume corrected mean grey matter perfusion (ml/100 g/min)	41.0 (7.23)	41.5 (6.3)	−0.79	0.43
FA	0.448 (0.02)	0.454 (0.01)	−1.57	0.12
MD[a]	0.727 (0.03)	0.725 (0.02)	0.97	0.33
AD[a]	1.11 (0.03)	1.11 (0.02)	0.12	0.91
RD[a]	0.533 (0.03)	0.528 (0.02)	1.3	0.2
WMH volume (cm^3)	0.063 (0.20)	0.049 (0.10)	0.17	0.987

[a] Mean and standard deviation for these DTI metrics have been multiplied by 10^3. WMH volume data was log transformed during the WMH analysis.

tract-based spatial statistics (TBSS) in FSL (v5.0.9, https://fsl.fmrib.ox.ac.uk/fsl/fslwiki/). This included motion- and eddy-current distortion-correction; rotation of the b matrix accordingly; motion quantification via root mean square deviation between each pair of realigned diffusion images and averaging over all pairs to create a single, 'relative' motion metric; brain extraction; and fitting a diffusion tensor to produce fractional anisotropy (FA), mean diffusivity (MD), axial diffusivity (AD, the principal diffusion eigenvalue), and radial diffusivity (RD, the mean of the second and third eigenvalues) images. Ten participants were excluded from DTI analyses: four with missing or truncated DTI sequences, three with absolute motion greater than two voxels (4 mm) and three with relative motion greater than three standard deviations of the mean, thus $n = 190$ ($n_{vlbw} = 141$, $n_{control} = 49$).

2.4.6. TBSS

FA images were aligned to a common space (FMRIB58_FA) using the nonlinear registration tool FNIRT. The mean FA image was created and thinned (FA > 0.2) to create a mean FA skeleton, representing the centres of principal white matter tracts common to all subjects. Participants' aligned FA images were then projected onto the study-specific FA skeleton image to create an FA skeleton in each subject. The nonlinear warps and skeleton projection were then applied to MD, AD, and RD images (Smith et al., 2006).

2.4.7. White matter Hyperintensities

White matter injury was quantified using the Lesion Segmentation Toolbox (Schmidt et al., 2012), which allows automatic detection of T2 hyperintensities based on the T2 FLAIR and T1-weighted images. This process produced a probabilistic white matter hyperintensity mask per person, which was normalized and smoothed (8 mm). In addition, we derived the total white matter hyperintensity (WMH) volume for each subject. Two participants were excluded from the analysis of WMH due to missing FLAIR sequences. Thus, sample size was $n = 198$ ($n_{vlbw} = 149$, $n_{control} = 49$).

2.5. Statistical analysis

Between group comparisons (VLBW vs full term controls) of global measures of total GM volume, mean GM perfusion, mean FA, MD, AD and RD along the skeleton, and log transformed WMH volume were conducted using multiple regression analyses in R (v3.0.2). Age at scan and sex were included in all models. ICV was included in the GM and WMH volume models, while relative motion was included in the FA, MD, AD and RD models. A chi-squared test was conducted to assess the distribution of male and female participants within the groups.

2.5.1. Voxelwise group analyses

Voxelwise group comparisons of regional GM volume and perfusion were performed using two sample *t*-tests in SPM12. Both models included age and sex as covariates, while ICV was an additional covariate in the GM volume model. Results were corrected for multiple comparisons using voxel-based family wise error rate ($p < 0.05$, cluster extent threshold = 0). Vertex-wise group comparisons of cortical thickness in Freesurfer (with age and sex) were corrected for multiple comparisons using precached clusterwise Monte Carlo simulation with 10,000 iterations (uncorrected $p < 0.001$ & corrected $p < 0.05$).

Voxelwise group comparisons of diffusion metrics (FA, MD, AD and RD) and WMH volume used a permutation-based inference tool for nonparametric statistical thresholding (FSL's 'randomise') (Winkler et al., 2014). Group differences (VLBW vs controls) were assessed with age and sex, with additional covariates of relative motion (DTI only) and ICV (WMH only). For each contrast, the null distribution was generated over 5000 permutations and the alpha level set at $p < 0.05$, corrected for multiple comparisons (family-wise error correction using threshold-free cluster enhancement, TFCE) (Smith and Nichols, 2009).

Within the VLBW group, relationships between birthweight and regional GM volume, perfusion and DTI measures were evaluated using permutation tests of correlation in FSL. All models included age and sex, while ICV was an additional covariate in the GM volume model and relative motion in the DTI models. A two-sample t-test was conducted in SPM12 to examine differences in GM volume between VLBW exposed to antenatal steroids (ANS) and VLBW who were not. Age, sex and evidence of intra-ventricular haemorrhage as indicated on cranial ultrasound were specified as covariates.

3. Results

3.1. Global results

Global MRI metrics are presented in Table 2. After accounting for age, sex and ICV, global GM volume was significantly lower in the VLBW group ($669 \pm 61\ cm^3$) relative to the control group ($723 \pm 62\ cm^3$, $t = 2.93$, $p < 0.01$). No differences in mean GM perfusion were observed between the groups, although a main effect of sex was observed ($t = -4.6$, $p < 0.001$), suggesting that males had mean GM perfusion of 4.4 ml/100 g/min less than their female counterparts. There were no significant differences in FA, MD, AD and RD averaged across the white matter skeleton between the two groups. However, males exhibited significantly lower mean RD than females.

3.2. Voxelwise results

3.2.1. GM volume

The VLBW group demonstrated smaller GM volumes than controls in the frontal lobe, within the orbital cortex, frontal pole and inferior frontal gyrus; the temporal lobe, including the superior, middle and inferior temporal gyri, planum temporale, Heschl's gyrus and temporal

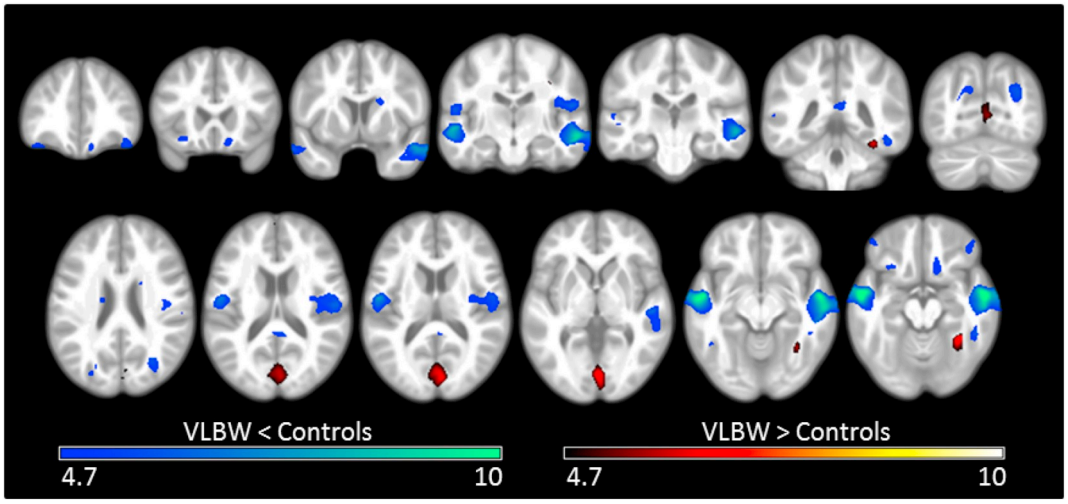

Fig. 1. Differences in regional GM volumes between VLBW and control adults.
Results of the voxel-based morphometric analysis, depicting regions of significant differences between VLBW and control groups in GM volume. Smaller volumes in VLBW relative to controls are illustrated in blue-green, while larger volumes are illustrated in red-yellow. Lighter colours reflect higher peak-level T statistics. Results are overlaid on the study-specific average structural image ($p < 0.05$ corrected for multiple comparisons using voxelwise family wise error rate). Specific regions exhibiting lower GM volume are listed in Supplementary Table S1. Slices displayed: y = 37, 21, 6, −16, −24, −42, −70; z = 24, 17, 14, 2, −10, −15. Images are displayed in neurological convention (left of the image is left of the brain). (For interpretation of the references to color in this figure legend, the reader is referred to the web version of this article.)

fusiform cortex. Significant regions were also observed in the occipital lobe, within the lateral occipital cortex and precuneus; the supramarginal gyrus of the parietal lobe, bilateral cingulate gyri and the left caudate nucleus. Greater GM volumes in VLBW adults relative to term control adults were observed in the frontal lobe, within the frontal pole and middle frontal gyrus; the temporal occipital fusiform cortex; the occipital lobe, within the occipital pole, lingual gyri, intracalcarine, supracalcarine and cuneal cortex; and within posterior cingulate gyri. As illustrated in Fig. 1, these between group differences in GM volumes showed a strong bilateral pattern (see also Supplementary Table S1).

3.2.2. Cortical thickness

Adults in the VLBW group had a thinner cerebral cortex than their term-born controls within limited, bilateral frontal, temporal and parietal cortices. Whereas, thicker cortex was observed within bilateral temporal and occipital regions (Fig. 2, Supplementary Table S2). Analysis of cortical thickness maps smoothed with a 20 mm FWHM Gaussian kernel showed significant differences in the same regions (Supplementary Fig. S1). Clusters were larger, as would be expected with a larger smoothing kernel.

3.2.3. Cerebral perfusion

A number of regions showed significantly less GM perfusion in the VLBW group relative to the control group. These included the right superior temporal gyrus, left lingual gyrus, and bilateral inferior temporal gyri, hippocampi and thalami (Fig. 3, Supplementary Table S3). A second model, including mean GM perfusion as an additional covariate, identified the same regions.

3.2.4. DTI

Fig. 4 and Supplementary Table S4 display tracts that showed significant DTI differences between groups. Those born VLBW were characterized by significantly lower FA bilaterally within the forceps major, inferior fronto-occipital and inferior longitudinal fasciculi, as well as within the posterior and superior corona radiata, and corpus callosum. VLBW participants also exhibited increased FA relative to controls in the right hemisphere only, within the superior longitudinal fasciculus, anterior, posterior and superior corona radiata, the inferior fronto-occipital fasciculus and corticospinal tract. The two groups did not differ significantly in terms of MD. Axial diffusivity was significantly lower within the corpus callosum (splenium), bilaterally within inferior longitudinal and inferior fronto-occipital fasciculi, the left forceps major and superior longitudinal fasciculus. Several regions exhibited greater AD in the VLBW group including the corpus callosum (genu and splenium), bilateral superior and posterior corona radiata, superior longitudinal fasciculi, corticospinal tracts and internal capsules, right anterior thalamic radiation and inferior fronto-occipital fasciculus, and the left anterior corona radiata. Greater RD in VLBW was found bilaterally within the corpus callosum (body), left forceps major and inferior fronto-occipital fasciculus. Many areas that demonstrated lower or higher FA in VLBW compared to controls showed changes in the same direction for AD. Lower FA and AD, and higher RD occurred predominantly within posterior WM tracts. The corpus callosum exhibited lower FA and high RD in VLBW relative to controls.

3.2.5. Neurosensory disabilities

Analyses of group differences in GM volume, cortical thickness, GM perfusion and DTI metrics excluding the six participants with moderate/severe neurosensory disability, showed minimal changes in significant regions and tracts compared to the results reported. The results of analyses excluding those with neurosensory disability are displayed in the Supplementary Material (Figs. S4 – S13).

3.2.6. White matter Hyperintensities

There were no significant differences (TFCE-corrected $p < 0.05$) in the size and distribution of WMH in VLBW vs Controls. However, the prevalence of WMHs was very low in this group of 27–29 year-olds. Most participants had no detectable WMHs.

3.3. Associations with birthweight within VLBW

3.3.1. Birthweight and GM volume

Decreasing birthweight was associated with lower GM volumes in the temporal lobe and various subcortical structures. Significant regions in the temporal lobe were largely isolated to the right hemisphere within superior and middle temporal gyri, planum temporale, planum

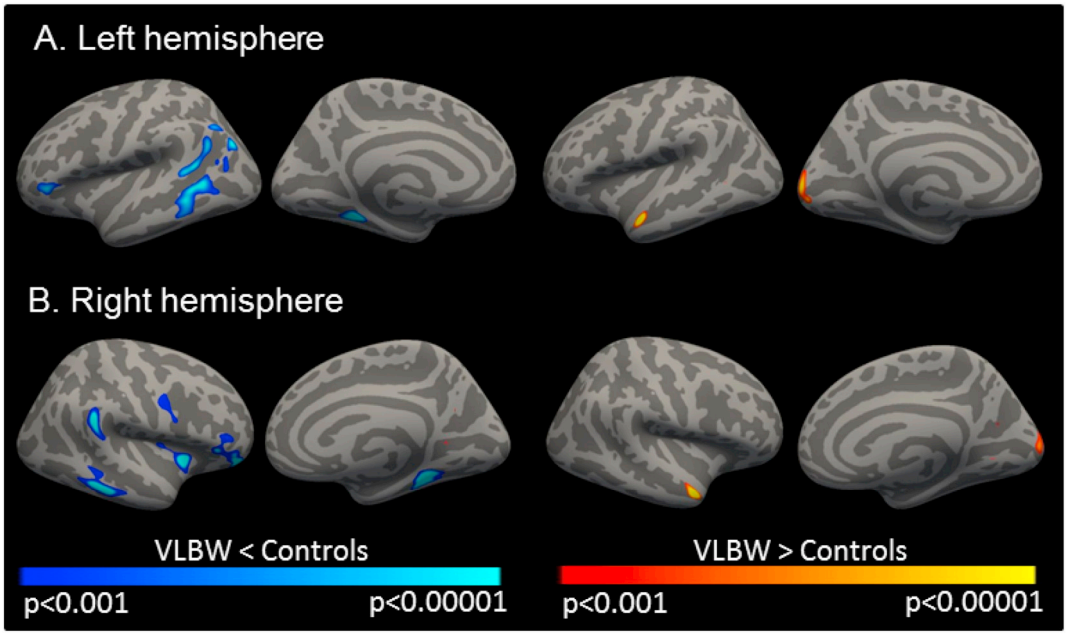

Fig. 2. VLBW adults demonstrate regions of thinner and thicker cortex relative to controls.
Results are overlaid on the reconstructed, inflated surface of the brain. Dark grey areas represent sulci, while light grey represent gyri. Clusters of significantly thinner cortex in VLBW relative to controls are depicted in blue and significantly thicker cortex is displayed in red-yellow within the A) left hemisphere and B) right hemisphere. Images display uncorrected p values within clusters that survived correction for multiple comparisons using precached clusterwise Monte Carlo simulation with 10,000 iterations (corrected $p < 0.05$). P values were adjusted for the analyses of left and right hemispheres. A smoothing kernel of FWHM 10 mm was used during the analysis. Specific regions demonstrating differences in cortical thickness between groups are listed in Supplementary Table S2. (For interpretation of the references to color in this figure legend, the reader is referred to the web version of this article.)

polare, amygdala, Heschl's gyrus, insular cortex, temporal pole, temporal occipital fusiform cortex and left temporal fusiform cortex. Subcortical structures included bilateral hippocampi and left caudate, putamen and pallidum. Decreasing birthweight was also associated with greater GM volumes in the frontal lobe, within the right frontal pole, middle frontal and inferior frontal gyri, and the left juxtapositional lobule cortex. Negative associations were also observed within the right middle temporal gyrus, and left cingulate and paracingulate gyri (Fig. 5, Supplementary Table S5).

3.3.2. *Birthweight and cortical thickness*

Positive correlations between birthweight and cortical thickness were observed within bilateral supramarginal gyri, limited regions within left temporal and right occipital cortices, and the right posterior cingulate gyrus (Supplementary Fig. S3 and Table S6).

3.3.3. *Birthweight and cerebral perfusion*

Within the VLBW group, decreasing birthweight was associated with lower GM perfusion in the temporal lobe, within bilateral Heschl's

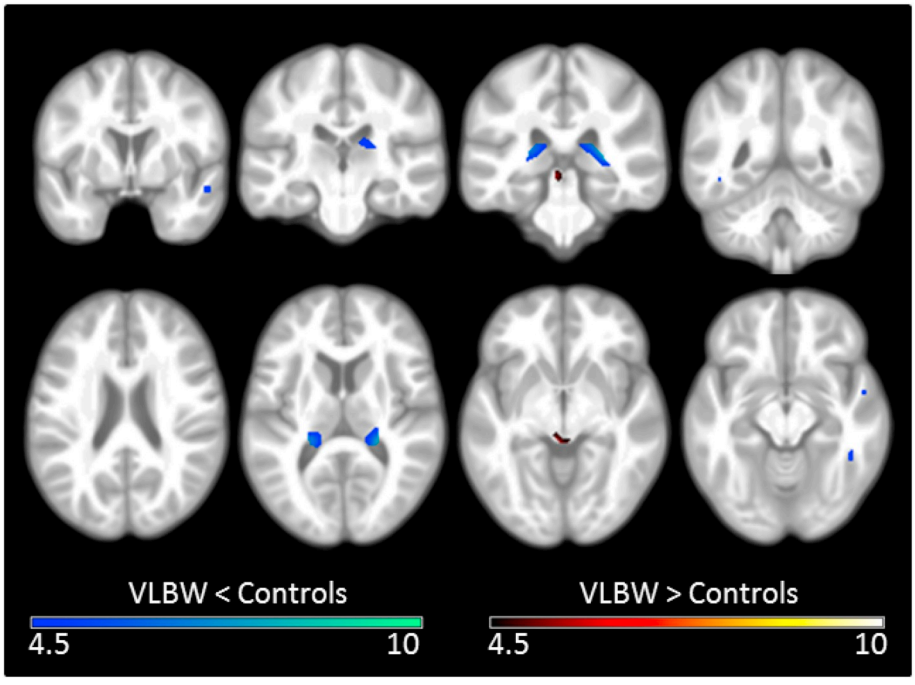

Fig. 3. Differences in regional GM perfusion between VLBW and control adults.
Results of the voxel-based morphometric analysis, depicting regions of significant differences between VLBW and control groups in GM perfusion. Regions of less perfusion in VLBW relative to controls are illustrated in blue-green, while greater perfusion is illustrated in red-yellow. Lighter colours reflect higher peak-level T statistics. Results are overlaid on the study-specific average structural image ($p < 0.05$ corrected for multiple comparisons using voxelwise family wise error rate). Specific regions exhibiting less GM perfusion are listed in Supplementary Table S3. Slices displayed: y = 1, −22, −32, −48; z = 23, 11, −5, −12. All images are displayed in neurological convention (left of the image is left of the brain). (For interpretation of the references to color in this figure legend, the reader is referred to the web version of this article.)

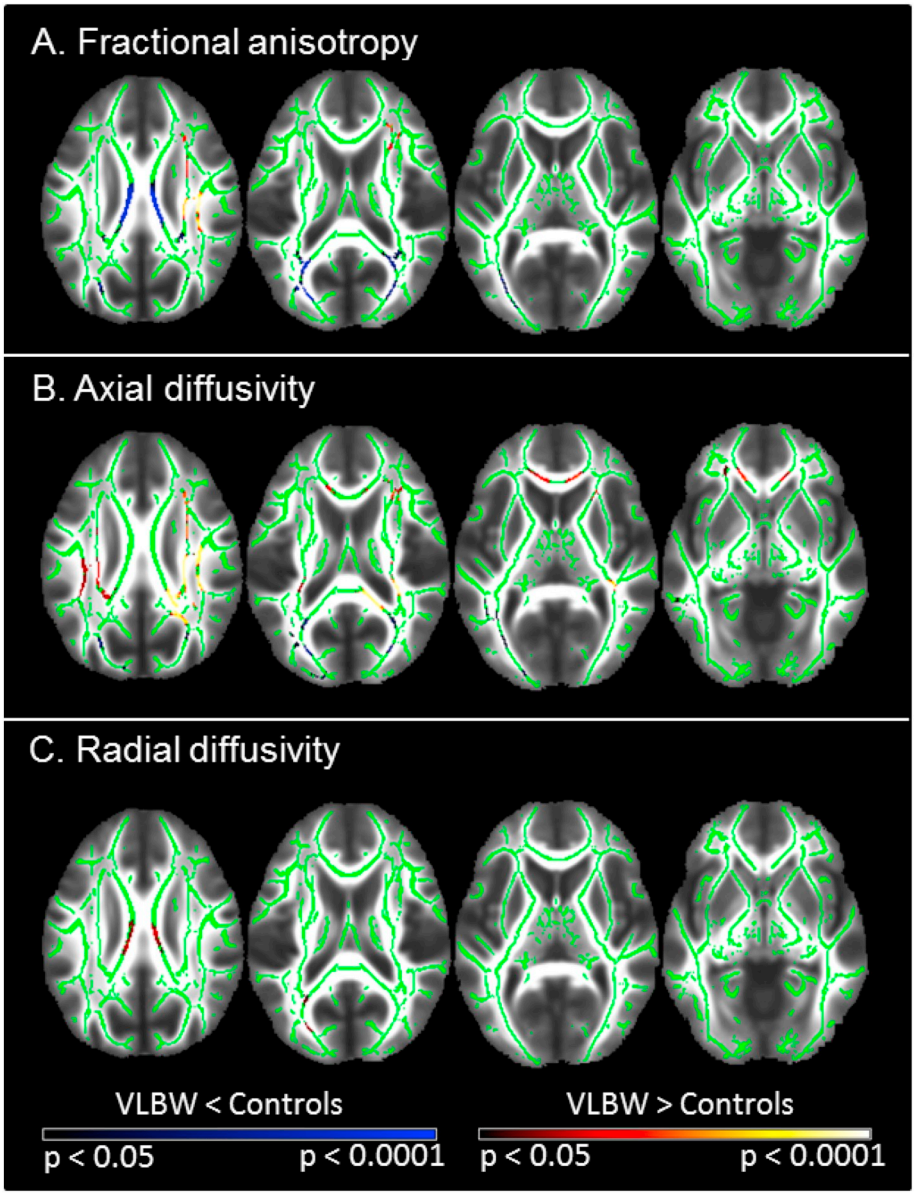

Fig. 4. Differences in DTI metrics between VLBW and control adults.
Results of the tract-based spatial statistics (TBSS) analysis demonstrate significant differences between groups in A) fractional anisotropy (FA), B) axial diffusivity and C) radial diffusivity. Lower values of diffusion metrics in VLBW relative to controls are displayed in blue, while higher values are shown in red-yellow. Lighter colours reflect smaller p-values. Results are overlaid on the mean FA image (TFCE-corrected for multiple comparisons $p < 0.05$). Specific regions exhibiting differences in DTI metrics are listed in Supplementary Table S4. Slices displayed: z = 27, 17, 7, −3, −13; neurological convention (left of the image is left of the brain). (For interpretation of the references to color in this figure legend, the reader is referred to the web version of this article.)

gyri and insular cortex, left temporal pole and middle temporal gyrus, the right amygdala and planum polare. Significant positive correlations were also observed within the right central opercular cortex and hippocampus (Fig. 5, Supplementary Table S7). No regions showed a significant negative association.

3.3.4. Birthweight and DTI

Birthweight was found to correlate with selected DTI metrics in several primary WM tracts (Fig. 6, Supplementary Table S8). Birthweight was positively correlated with FA within the corpus callosum (body and splenium), bilaterally within the posterior thalamic radiation, external capsule, inferior and superior longitudinal fasciculi. Positive correlations were also found within the right anterior thalamic radiation, cingulum, fornix, internal capsule, inferior fronto-occipital and uncinate fasciculi, and the left forceps major. Positive correlations between birthweight and AD were found bilaterally within inferior longitudinal fasciculi, forceps major, external and internal capsules, fornix, and cerebral peduncles. Positive correlations were also noted within the right cingulum, superior longitudinal and uncinate fasciculi, and the left anterior thalamic radiation. Birthweight correlated negatively with RD within the left posterior thalamic radiation, forceps major, superior longitudinal fasciculus, posterior corona radiata and the corpus callosum (splenium).

3.3.5. GM volume and antenatal steroids

No differences in GM volume were observed between VLBW participants exposed to ANS and those who were not.

4. Discussion

Pervasive differences in GM volumes, cortical thickness, GM perfusion, and DTI metrics were observed between young adults born VLBW and term-born controls. Furthermore, within the VLBW group, clear associations were found between birthweight and a range of adult brain outcomes assessed using multiple imaging methods.

4.1. GM volume

The results of the present study are consistent with previous findings showing that children, adolescents and adults born VLBW and/or very preterm, have less GM volume than their same age term-born peers. Reductions in GM volume have previously been reported in frontal

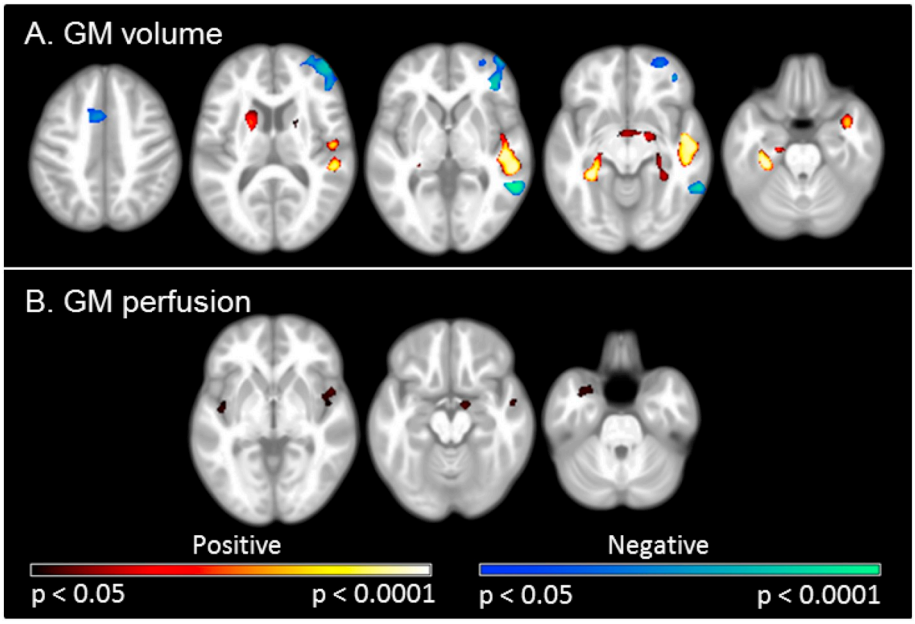

Fig. 5. Associations of birthweight with GM volume and perfusion in VLBW adults.
Results of permutation tests of correlation in FSL depicting correlations between birthweight and A) grey matter (GM) volume, and B) GM perfusion. Regions demonstrating positive correlations with birthweight are depicted in red-yellow, while negative correlations are displayed in blue-green. Lighter colours reflect smaller p-values. Results are overlaid on the study-specific average structural image ($p < 0.05$ corrected for multiple comparisons using TFCE). Specific regions exhibiting correlations between birthweight and GM volume are listed in Supplementary Table S5, while correlations between birthweight and GM perfusion are listed in Supplementary Table S7. Slices displayed (A): $z = 46, 12, 1, -9, -24$; (B): $z = -2, -15, -28$. All slices are displayed in neurological convention (left of the image is left of the brain). (For interpretation of the references to color in this figure legend, the reader is referred to the web version of this article.)

regions, including the inferior frontal gyrus (Nosarti et al., 2008) and premotor region (Peterson et al., 2000), temporal cortices, including superior (Nosarti et al., 2008), middle (Nosarti et al., 2008; Soria-Pastor et al., 2009) and inferior temporal gyri (Nosarti et al., 2008), midtemporal (Peterson et al., 2000), superior and medial temporal cortices (Nagy et al., 2009). Also in accordance with our results, smaller GM volumes have been found within the precuneus (Nosarti et al., 2008), parieto-occipital regions (Peterson et al., 2000) and subcortical

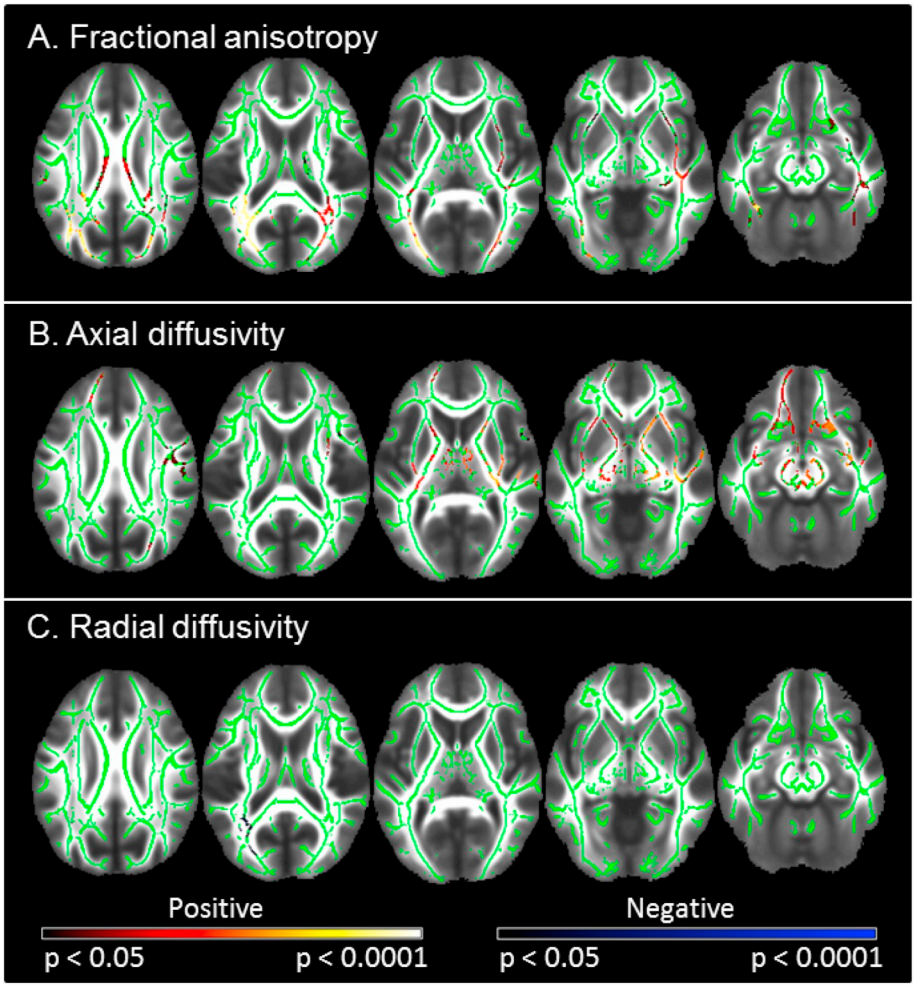

Fig. 6. Associations between birthweight and DTI metrics in VLBW adults.
Results of permutation tests of correlation in FSL demonstrate correlations between birthweight and A) fractional anisotropy (FA), B) axial diffusivity, and C) radial diffusivity, within principle white matter tracts. Areas of positive correlation are depicted in red-yellow, while negative correlations are represented in blue. Lighter colours reflect smaller p-values. Results are overlaid on the mean FA image (TCFE-corrected for multiple comparisons $p < 0.05$). Specific regions exhibiting correlations between birthweight and DTI metrics and are listed in Supplementary Table S8. Slices displayed: $z = 27, 17, 7, -3, -13$; neurological convention (left of the image is left of the brain). (For interpretation of the references to color in this figure legend, the reader is referred to the web version of this article.)

GM (Taylor et al., 2011), particularly the caudate nuclei (Abernethy et al., 2002; Nosarti et al., 2008; Peterson et al., 2000). Additionally, the temporo-parietal junction has been reported to show thinner cortex in VLBW young adults (Rimol et al., 2019). However, while MRI can provide information about the volume of GM in a particular region, it does not distinguish the underlying cause. One explanation for our findings may be that disruptions in the formation of connections between brain regions in preterm neonates (Ball et al., 2013) might alter subsequent brain development and reduce synaptogenesis, which in turn, could lead to smaller GM volumes and thinner cortex (Huttenlocher and Dabholkar, 1997). The widespread reductions in GM volume of those born VLBW might reflect the vastly interconnected nature of the brain and possibly the downstream impacts of primary WM lesion/s on more widely distributed regions of the brain (Hack and Taylor, 2000).

Furthermore, we found several regions that exhibited greater GM volume within our VLBW cohort relative to control subjects. A follow-up study of 12-year-old VP participants, who were imaged with the same MRI scanner as the present study, found increased GM volumes within the medial occipital cortex, including the supracalcarine and intracalcarine gyri, and the anterior cingulate gyrus, compared with controls (Lean et al., 2017). Our findings of increased GM volume are consistent with those of Lean et al. (2017). However, we found the posterior, rather than anterior, cingulate gyrus to be significant. Our results also support findings of greater GM volume in other preterm and low birthweight populations within frontal (Kesler et al., 2004) and temporal (Allin et al., 2004; Nosarti et al., 2008) cortices, specifically within fusiform cortex, middle frontal, lingual and cingulate gyri (Nosarti et al., 2008). Thicker cortex has also been reported within frontal and occipital regions of VLBW young adults (Rimol et al., 2019). Kesler et al. (2004), speculated that their findings of increased GM volume within frontal regions may be related to delayed synaptic pruning in these areas, based on evidence that the frontal lobe is the last to undergo maturation. Delayed synaptic pruning may be a potential explanation for the regions of increased GM volume observed in our VLBW group. However, there is conflicting evidence regarding the progression of cortical GM development during childhood and adolescence. Gogtay et al. (2004) found that the temporal lobe was the last to mature, preceded by regions of the frontal lobe. Conversely, the occipital lobe has also been indicated as being the last region to reach peak GM volume (Giedd et al., 1999). Based on evidence for late maturation of the temporal and occipital lobes, it is possible that the larger GM volumes in the temporal occipital fusiform cortex, intracalcarine and supracalcarine cortices observed in our VLBW group may not simply reflect greater volume or growth, but rather a delayed decrease in volume, mediated by delayed synaptic pruning. Although this might seem unlikely given the widely accepted notion that synaptic pruning finishes by the end of adolescence (Huttenlocher, 1979), new evidence does suggest that elimination of dendritic spines of pyramidal neurons in the prefrontal cortex can persist into the third decade of life (Petanjek et al., 2011).

4.2. GM perfusion

Few studies have investigated cerebral perfusion using arterial spin labelling MRI in low birthweight or preterm populations. The majority of studies have focused on cerebral perfusion in infants and have revealed mixed findings. Miranda et al. (2006), compared cerebral perfusion in preterm and term neonates, using arterial spin labelling and found that cerebral perfusion was greater in preterm than term control infants. However, Kehrer et al. (2003), used colour duplex sonography of the extracranial cerebral arteries to demonstrate lower cerebral perfusion in those born preterm, in addition to a pattern of increasing perfusion with increasing postmenstrual age. With the known plasticity of the brain and the development and maturation it undergoes over the years, it is hard to conjecture how differences in cerebral perfusion between preterm and term infants may relate to the differences we observed in young adults. The values we obtained for global GM perfusion in VLBW (50.6 ± 8.8) and control (51.6 ± 7.6) adults are consistent with previously documented perfusion values in similar age groups (Biagi et al., 2007; Lassen, 1985; Wang et al., 2003). While we did not find evidence for a significant difference in global GM perfusion between groups, we did observe lower regional GM perfusion in VLBW participants within the temporal lobe, lingual gyrus, bilateral hippocampi and thalami. Reduced cerebral perfusion within small regions of the right inferior and superior temporal gyri corresponds with reductions in GM volume. In contrast to reduced GM volume and perfusion within the superior temporal gyrus, cortical thickness was found to be greater bilaterally in this region in the VLBW cohort. Overall, we do not see many specific regions which show differences in both GM perfusion, and GM volume and cortical thickness.

4.3. White matter

Concerning WM, differences in FA between VLBW and controls were found within tracts previously documented to show changes in measures of diffusion, including decreased FA in the forceps major (Constable et al., 2008), corpus callosum (splenium) (Allin et al., 2011; Constable et al., 2008; Vangberg et al., 2006) inferior longitudinal fasciculi (Eikenes et al., 2011; Skranes et al., 2007) and inferior fronto-occipital fasciculi (Constable et al., 2008; Eikenes et al., 2011; Skranes et al., 2007). Greater FA was also observed in tracts consistent with previous studies, including the right corticospinal tract (Feldman et al., 2012), superior longitudinal (Rimol et al., 2019) and inferior fronto-occipital fasciculi (Allin et al., 2011; Feldman et al., 2012). Interpretation of FA is complex as it can be affected by numerous properties of WM tracts, including the extent of myelination of axons, membrane permeability, axon density, and the organisation of fibres (Vangberg et al., 2006). The reductions in FA observed in the VLBW group are likely to be related to one or more of these properties which influence the integrity of WM. Interpreting increased FA within VLBW is even more difficult. It is possible that increases in FA are the result of preferential degradation of a single tract within areas of crossing fibres. For example, Groeschel et al. (2014), showed that a relative increase in FA can occur when the FA of an underlying crossing tract in a given voxel is reduced. While it is possible that this scenario may contribute to the regions of increased FA observed in those born VLBW, our results are in line with previous findings reported in VLBW and preterm populations (Allin et al., 2004; Kesler et al., 2004; Nosarti et al., 2008), and tend to indicate a change in underlying structure. In this case, increased FA may reflect the brain's potential for neuroplasticity and the ability to compensate for distant and connected regions or tracts that may show disruption in development, as a result of VLBW or premature birth (Allin et al., 2011).

4.4. Combining results across multiple imaging metrics

Combining our results across multiple imaging sequences and processing techniques reveals some interesting patterns. As previously mentioned, we speculate that observed temporal and occipital regions of greater GM volume may reflect a delay in synaptic pruning in the VLBW cohort. Additionally, we also found an increase in cortical thickness in regions of the temporal and occipital cortices. Evidence suggests that in normal development, decreasing cortical thickness may reflect increased myelination, producing an artefactual shift in the GM/WM boundary (Sowell et al., 2004). Given this finding, the increases in cortical thickness seen in the VLBW group may reflect a reduction in the normal increase in myelination. This idea is further supported by our WM findings of lower FA and AD, and higher RD within posterior WM tracts, particularly the forceps major which connects bilateral occipital lobes. The spatial proximity of increased GM volume and cortical thickness and reduced WM integrity suggests that maturation in these

areas may involve both synaptic pruning and increased myelination. We may be seeing the effects of disruption to both maturation processes in VLBW adults.

Another apparent pattern across imaging metrics is the consistent appearance of the temporal lobe as a region showing significant differences between groups. Whilst we have found differences within all lobes and many subcortical structures across various imaging metrics, between group differences within the temporal lobe were evident across all imaging modalities and statistical analyses. This may suggest that the temporal lobe is particularly susceptible to disruption in development following preterm birth. A study of preterm children found increased gyrification exclusively in bilateral temporal lobes (Kesler et al., 2006). Furthermore, Kesler et al. (2006) found left temporal gyrification was negatively correlated with left temporal GM volume and suggested that cortical development in the temporal lobe may be differentially affected by preterm birth. A primate animal model has also demonstrated that injury to the preterm brain commonly occurs in regions associated with the temporal lobe (Dieni et al., 2004). Further analysis of the neurobehavioral correlates of these findings will be important.

4.5. Associations with birthweight

Within our VLBW cohort, birthweight showed significant associations with measures of GM volume, perfusion and DTI metrics across numerous brain regions and WM tracts. This is consistent with, and extends, earlier studies showing that birthweight was positively associated with later GM volume (Nagy et al., 2009; Soria-Pastor et al., 2009) within numerous brain regions. Concerning associations between birthweight and FA, our results are also similar to those of Eikenes et al. (2011) who found significant positive correlations between birthweight and FA within the cingulum, superior longitudinal, inferior fronto-occipital and inferior longitudinal fasciculi, forceps major, uncinate fasciculi, and corpus callosum. Extending these results, we also found that lower birthweight was associated with reduced GM volume and perfusion, lower FA and AD, and elevated RD within certain regions. Collectively, these findings suggest that lower birthweight or earlier prematurity is associated, at least at the group level, with greater and/or more extensive alterations in brain structure and function that are observable into early adulthood (Nagy et al., 2009; Nosarti et al., 2008; Peterson et al., 2000).

4.6. Strengths and limitations

Strengths of the study include the national cohort from which participants were selected to complete MRI scanning, and the consolidation of findings from multiple imaging measures within a sample of VLBW adults followed-up from birth. A potential limitation may be that infants were classified by birthweight, rather than gestational age. However, in the 1980s birthweight was routinely used rather than gestational age to define preterm populations (Hack and Fanaroff, 1988). While birthweight does correlate strongly with gestational age, the latter may provide more information about an infant's developmental state. Nevertheless, our results remain consistent with those of other studies, whether participants were classified by birthweight or gestational age (Nagy et al., 2009; Nosarti et al., 2008). Mean age at scan of those born VLBW was slightly higher than controls; therefore, age was accounted for in all analyses. We investigated both grey matter volume and cortical thickness. While derived from the same T1-weighted image, the two methods investigate two different properties and may provide differing results. Smoothing may contribute to these potential differences. In volume-based methods, data is smoothed with a three-dimensional isotropic Gaussian kernel, whereas surface-based methods employ a two-dimensional kernel. Due to cortical folding in volumetric data, neighbouring voxels in 3D space may not be spatially proximate in the corresponding 2D cortical surface. Thus, in volumetric analyses voxels may be smoothed that are not truly spatially proximate. This has the potential to alter the signal and therefore, subsequent results. It has been shown that smoothing on the surface preserves signal better than smoothing of volumes (Anticevic et al., 2008). Despite this, the GM volume and cortical thickness results presented in this paper remain consistent with findings in other studies of VLBW. Indeed, group differences might have been even larger than our results suggest, if the sample had not included proportionally more VLBW participants with better outcomes due to the differing rates of moderate/severe neurosensory disability at age 7–8 of VLBW participants scanned (4%) and not scanned (14%). However, oversampling of extremely preterm (< 28 weeks gestation) participants for scanning could also have altered the proportion of VLBW with better outcomes, affecting generalizability of results to all VLBW survivors. Further replication will be important.

5. Conclusions

This study examined the neurological outcomes of a national cohort of adults born VLBW using multiple imaging methods, spanning measures of GM volume, cortical thickness, perfusion and WM integrity. Findings revealed clear between group differences between VLBW and healthy term-born control adults across all four imaging methods; thus, suggesting that very preterm birth has widespread effects on the neonatal brain that persist well into adulthood. Additionally, there was clear evidence of converging results across imaging modalities, indicating vulnerability of specific brain regions, particularly the temporal lobe. Finally, we also found that lower birthweight or greater prematurity tended to be associated with higher levels of long-term neuropathology, including greater alterations/abnormalities in GM volume, cortical thickness, perfusion and WM integrity. Further examination of the adult functional significance of these findings will be an important next step, in addition to understanding the effects of aging on the potentially vulnerable brains of very preterm/VLBW survivors.

Funding

The study was funded by a project grant from the Health Research Council of New Zealand (12-129) with additional funding from Cure Kids, and project grants from the Child Health Research Foundation (CHRF 5040 and CHRF 5041).

Acknowledgements

We thank all of the young participants for their willingness to take part in this study. We are grateful to Julia Martin, the Project Manager, and Dr. Ross Keenan and Gareth Leeper who contributed to data collection.

Appendix A. Supplementary data

Supplementary data to this article can be found online at https://doi.org/10.1016/j.nicl.2019.101780.

References

Abernethy, L., Palaniappan, M., Cooke, R., 2002. Quantitative magnetic resonance imaging of the brain in survivors of very low birth weight. Arch. Dis. Child. 87, 279–283.
Allin, M., Henderson, M., Suckling, J., Nosarti, C., Rushe, T., Fearon, P., ... Murray, R., 2004. Effects of very low birthweight on brain structure in adulthood. Dev. Med. Child Neurol. 46, 46–53.
Allin, M., Kontis, D., Walshe, M., Wyatt, J., Barker, G.J., Kanaan, R.A., ... Nosarti, C., 2011. White matter and cognition in adults who were born preterm. PLoS One 6, e24525.
Anderson, P.J., Cheong, J.L., Thompson, D.K., 2015. The Predictive Validity of Neonatal MRI for Neurodevelopmental Outcome in Very Preterm Children. (Paper presented at the Seminars in perinatology).
Anticevic, A., Dierker, D.L., Gillespie, S.K., Repovs, G., Csernansky, J.G., Van Essen, D.C.,

Barch, D.M., 2008. Comparing surface-based and volume-based analyses of functional neuroimaging data in patients with schizophrenia. Neuroimage 41, 835–848.
Ashburner, J., Friston, K.J., 2005. Unified segmentation. Neuroimage 26, 839–851.
Back, S.A., 2017. White matter injury in the preterm infant: pathology and mechanisms. Acta Neuropathol. 134, 331–349.
Ball, G., Boardman, J.P., Aljabar, P., Pandit, A., Arichi, T., Merchant, N., ... Counsell, S.J., 2013. The influence of preterm birth on the developing thalamocortical connectome. Cortex 49, 1711–1721.
Belfort, M.B., Ehrenkranz, R.A., 2017. Neurodevelopmental outcomes and nutritional strategies in very low birth weight infants. In: Paper presented at the Seminars in Fetal and Neonatal Medicine.
Biagi, L., Abbruzzese, A., Bianchi, M.C., Alsop, D.C., Del Guerra, A., Tosetti, M., 2007. Age dependence of cerebral perfusion assessed by magnetic resonance continuous arterial spin labeling. J. Magn. Reson. Imaging 25, 696–702.
Bjuland, K.J., Løhaugen, G.C.C., Martinussen, M., Skranes, J., 2013. Cortical thickness and cognition in very-low-birth-weight late teenagers. Early Hum. Dev. 89, 371–380.
Bjuland, K.J., Rimol, L.M., Løhaugen, G.C., Skranes, J., 2014. Brain volumes and cognitive function in very-low-birth-weight (VLBW) young adults. Eur. J. Paediatr. Neurol. 18, 578–590.
Brew, N., Walker, D., Wong, F.Y., 2014. Cerebral vascular regulation and brain injury in preterm infants. Am. J. Phys. Regul. Integr. Comp. Phys. 306, R773–R786.
Brummelte, S., Grunau, R.E., Chau, V., Poskitt, K.J., Brant, R., Vinall, J., ... Miller, S.P., 2012. Procedural pain and brain development in premature newborns. Ann. Neurol. 71, 385–396.
Chételat, G., Desgranges, B., Landeau, B., Mézenge, F., Poline, J., de La Sayette, V., ... Baron, J.-C., 2007. Direct voxel-based comparison between grey matter hypometabolism and atrophy in Alzheimer's disease. Brain 131, 60–71.
Constable, R.T., Ment, L.R., Vohr, B.R., Kesler, S.R., Fulbright, R.K., Lacadie, C., ... Schafer, R.J., 2008. Prematurely born children demonstrate white matter microstructural differences at 12 years of age, relative to term control subjects: an investigation of group and gender effects. Pediatrics 121, 306–316.
Cuadra, M.B., Cammoun, L., Butz, T., Cuisenaire, O., Thiran, J.-P., 2005. Comparison and validation of tissue modelization and statistical classification methods in T1-weighted MR brain images. IEEE Trans. Med. Imaging 24, 1548–1565.
Dai, W., Garcia, D., de Bazelaire, C., Alsop, D.C., 2008. Continuous flow-driven inversion for arterial spin labeling using pulsed radio frequency and gradient fields. Magn. Reson. Med. 60, 1488–1497.
Darlow, B.A., Horwood, L.J., Woodward, L.J., Elliott, J.M., Troughton, R.W., Elder, M.J., ... Keenan, R., 2015. The New Zealand 1986 very low birth weight cohort as young adults: mapping the road ahead. BMC Pediatr. 15, 90.
de Kieviet, J.F., Zoetebier, L., Van Elburg, R.M., Vermeulen, R.J., Oosterlaan, J., 2012. Brain development of very preterm and very low-birthweight children in childhood and adolescence: a meta-analysis. Dev. Med. Child Neurol. 54, 313–323.
Dieni, S., Inder, T., Yoder, B., Briscoe, T., Camm, E., Egan, G., ... Rees, S., 2004. The pattern of cerebral injury in a primate model of preterm birth and neonatal intensive care. J. Neuropathol. Exp. Neurol. 63, 1297–1309.
Eikenes, L., Løhaugen, G.C., Brubakk, A.-M., Skranes, J., Håberg, A.K., 2011. Young adults born preterm with very low birth weight demonstrate widespread white matter alterations on brain DTI. Neuroimage 54, 1774–1785.
Feldman, H.M., Lee, E.S., Loe, I.M., Yeom, K.W., GRILL-SPECTOR, K., Luna, B., 2012. White matter microstructure on diffusion tensor imaging is associated with conventional magnetic resonance imaging findings and cognitive function in adolescents born preterm. Dev. Med. Child Neurol. 54, 809–814.
Fyfe, K.L., Yiallourou, S.R., Wong, F.Y., Horne, R.S., 2014. The development of cardiovascular and cerebral vascular control in preterm infants. Sleep Med. Rev. 18, 299–310.
Giedd, J.N., Blumenthal, J., Jeffries, N.O., Castellanos, F.X., Liu, H., Zijdenbos, A., ... Rapoport, J.L., 1999. Brain development during childhood and adolescence: a longitudinal MRI study. Nat. Neurosci. 2, 861–863.
Gogtay, N., Giedd, J.N., Lusk, L., Hayashi, K.M., Greenstein, D., Vaituzis, A.C., Toga, A.W., 2004. Dynamic mapping of human cortical development during childhood through early adulthood. Proc. Natl. Acad. Sci. U. S. A. 101, 8174–8179.
Gonzalez-Redondo, R., García-García, D., Clavero, P., Gasca-Salas, C., García-Eulate, R., Zubieta, J.L., ... Rodríguez-Oroz, M.C., 2014. Grey matter hypometabolism and atrophy in Parkinson's disease with cognitive impairment: a two-step process. Brain 137, 2356–2367.
Groeschel, S., Tournier, J.-D., Northam, G.B., Baldeweg, T., Wyatt, J., Vollmer, B., Connelly, A., 2014. Identification and interpretation of microstructural abnormalities in motor pathways in adolescents born preterm. NeuroImage 87, 209–219.
Grunau, R.E., Holsti, L., Peters, J.W., 2006. Long-Term Consequences of Pain in Human Neonates. (Paper presented at the Seminars in Fetal and Neonatal Medicine).
Hack, M., Fanaroff, A.A., 1988. How small is too small? Considerations in evaluating the outcome of the tiny infant. Clin. Perinatol. 15, 773–788.
Hack, M., Taylor, H.G., 2000. Perinatal brain injury in preterm infants and later neurobehavioral function. Jama 284, 1973–1974.
Hansen, T., Brezova, V., Eikenes, L., Håberg, A., Vangberg, T., 2015. How does the accuracy of intracranial volume measurements affect normalized brain volumes? Sample size estimates based on 966 subjects from the HUNT MRI cohort. Am. J. Neuroradiol. 36, 1450–1456.
Huttenlocher, P.R., 1979. Synaptic density in human frontal cortex-developmental changes and effects of aging. Brain Res. 163, 195–205.
Huttenlocher, P.R., Dabholkar, A.S., 1997. Regional differences in synaptogenesis in human cerebral cortex. J. Comp. Neurol. 387, 167–178.
Kapellou, O., Counsell, S.J., Kennea, N., Dyet, L., Saeed, N., Stark, J., Hajnal, J., 2006. Abnormal cortical development after premature birth shown by altered allometric scaling of brain growth. PLoS Med. 3, e265.
Kehrer, M., Krägeloh-Mann, I., Goelz, R., Schöning, M., 2003. The development of cerebral perfusion in healthy preterm and term neonates. Neuropediatrics 34, 281–286.
Kesler, S.R., Ment, L.R., Vohr, B., Pajot, S.K., Schneider, K.C., Katz, K.H., ... Reiss, A.L., 2004. Volumetric analysis of regional cerebral development in preterm children. Pediatr. Neurol. 31, 318–325.
Kesler, S.R., Vohr, B., Schneider, K.C., Katz, K.H., Makuch, R.W., Reiss, A.L., Ment, L.R., 2006. Increased temporal lobe gyrification in preterm children. Neuropsychologia 44, 445–453.
Keunen, K., Counsell, S.J., Benders, M.J., 2017. The emergence of functional architecture during early brain development. Neuroimage 160, 2–14.
Kinney, H.C., Volpe, J.J., 2018. Encephalopathy of Prematurity: Neuropathology Volpe's Neurology of the Newborn. Elsevier, pp. 389–404.
Lassen, N.A., 1985. Normal Average Value of Cerebral Blood Flow in Younger Adults is 50 ml/100 g/min. SAGE Publications Sage UK, London, England.
Lean, R.E., Melzer, T.R., Bora, S., Watts, R., Woodward, L.J., 2017. Attention and regional gray matter development in very preterm children at age 12 years. J. Int. Neuropsychol. Soc. 1–12.
Li, K., Sun, Z., Han, Y., Gao, L., Yuan, L., Zeng, D., 2015. Fractional anisotropy alterations in individuals born preterm: a diffusion tensor imaging meta-analysis. Dev. Med. Child Neurol. 57, 328–338.
Liang, X., Connelly, A., Calamante, F., 2013. Improved partial volume correction for single inversion time arterial spin labeling data. Magn. Reson. Med. 69, 531–537.
Mahdi, E., Bouyssi-Kobar, M., Jacobs, M., Murnick, J., Chang, T., Limperopoulos, C., 2018. Cerebral perfusion is perturbed by preterm birth and brain injury. Am. J. Neuroradiol. 39, 1330–1335.
Martinussen, M., Fischl, B., Larsson, H., Skranes, J., Kulseng, S., Vangberg, T., ... Dale, A., 2005. Cerebral cortex thickness in 15-year-old adolescents with low birth weight measured by an automated MRI-based method. Brain 128, 2588–2596.
Miranda, M.J., Olofsson, K., Sidaros, K., 2006. Noninvasive measurements of regional cerebral perfusion in preterm and term neonates by magnetic resonance arterial spin labeling. Pediatr. Res. 60, 359–363.
Moeskops, P., Benders, M.J., Kersbergen, K.J., Groenendaal, F., de Vries, L.S., Viergever, M.A., Išgum, I., 2015. Development of cortical morphology evaluated with longitudinal MR brain images of preterm infants. PLoS One 10, e0131552.
Nagy, Z., Westerberg, H., Skare, S., Andersson, J.L., Lilja, A., Flodmark, O., ... Forssberg, H., 2003. Preterm children have disturbances of white matter at 11 years of age as shown by diffusion tensor imaging. Pediatr. Res. 54, 672–679.
Nagy, Z., Ashburner, J., Andersson, J., Jbabdi, S., Draganski, B., Skare, S., ... Lagercrantz, H., 2009. Structural correlates of preterm birth in the adolescent brain. Pediatrics 124, e964–e972.
Nagy, Z., Lagercrantz, H., Hutton, C., 2010. Effects of preterm birth on cortical thickness measured in adolescence. Cereb. Cortex 21, 300–306.
Nosarti, C., Al-Asady, M.H., Frangou, S., Stewart, A.L., Rifkin, L., Murray, R.M., 2002. Adolescents who were born very preterm have decreased brain volumes. Brain 125, 1616–1623.
Nosarti, C., Giouroukou, E., Healy, E., Rifkin, L., Walshe, M., Reichenberg, A., ... Murray, R.M., 2008. Grey and white matter distribution in very preterm adolescents mediates neurodevelopmental outcome. Brain 131, 205–217.
Nosarti, C., Nam, K.W., Walshe, M., Murray, R.M., Cuddy, M., Rifkin, L., Allin, M., 2014. Preterm birth and structural brain alterations in early adulthood. NeuroImage 6, 180–191.
Petanjek, Z., Judaš, M., Šimić, G., Rašin, M.R., Uylings, H.B., Rakic, P., Kostović, I., 2011. Extraordinary neoteny of synaptic spines in the human prefrontal cortex. Proc. Natl. Acad. Sci. 108, 13281–13286.
Peterson, B.S., Vohr, B., Staib, L.H., Cannistraci, C.J., Dolberg, A., Schneider, K.C., ... Anderson, A.W., 2000. Regional brain volume abnormalities and long-term cognitive outcome in preterm infants. Jama 284, 1939–1947.
Rajapakse, J.C., Giedd, J.N., Rapoport, J.L., 1997. Statistical approach to segmentation of single-channel cerebral MR images. IEEE Trans. Med. Imaging 16, 176–186.
Raju, T.N., Buist, A.S., Blaisdell, C.J., Moxey-Mims, M., Saigal, S., 2017. Adults born preterm: a review of general health and system-specific outcomes. Acta Paediatr. 106, 1409–1437.
Rimol, L.M., Botellero, V.L., Bjuland, K.J., Løhaugen, G.C., Lydersen, S., Evensen, K.A.I., ... Martinussen, M., 2019. Reduced white matter fractional anisotropy mediates cortical thickening in adults born preterm with very low birthweight. NeuroImage 188, 217–227.
Schmidt, P., Gaser, C., Arsic, M., Buck, D., Förschler, A., Berthele, A., ... Zimmer, C., 2012. An automated tool for detection of FLAIR-hyperintense white-matter lesions in multiple sclerosis. Neuroimage 59, 3774–3783.
Skranes, J., Vangberg, T., Kulseng, S., Indredavik, M., Evensen, K., Martinussen, M., ... Brubakk, A.-M., 2007. Clinical findings and white matter abnormalities seen on diffusion tensor imaging in adolescents with very low birth weight. Brain 130, 654–666.
Smith, S.M., Nichols, T.E., 2009. Threshold-free cluster enhancement: addressing problems of smoothing, threshold dependence and localisation in cluster inference. Neuroimage 44, 83–98.
Smith, S.M., Jenkinson, M., Johansen-Berg, H., Rueckert, D., Nichols, T.E., Mackay, C.E., ... Matthews, P.M., 2006. Tract-based spatial statistics: voxelwise analysis of multi-subject diffusion data. Neuroimage 31, 1487–1505.
Soria-Pastor, S., Padilla, N., Zubiaurre-Elorza, L., Ibarretxe-Bilbao, N., Botet, F., Costas-Moragas, C., ... Junque, C., 2009. Decreased regional brain volume and cognitive impairment in preterm children at low risk. Pediatrics 124, e1161–e1170.
Sowell, E.R., Thompson, P.M., Leonard, C.M., Welcome, S.E., Kan, E., Toga, A.W., 2004. Longitudinal mapping of cortical thickness and brain growth in normal children. J. Neurosci. 24, 8223–8231.
Taylor, H.G., Filipek, P.A., Juranek, J., Bangert, B., Minich, N., Hack, M., 2011. Brain volumes in adolescents with very low birth weight: effects on brain structure and

associations with neuropsychological outcomes. Dev. Neuropsychol. 36, 96–117.
Tohka, J., Zijdenbos, A., Evans, A., 2004. Fast and robust parameter estimation for statistical partial volume models in brain MRI. Neuroimage 23, 84–97.
Vangberg, T.R., Skranes, J., Dale, A.M., Martinussen, M., Brubakk, A.-M., Haraldseth, O., 2006. Changes in white matter diffusion anisotropy in adolescents born prematurely. Neuroimage 32, 1538–1548.
Wang, J., Licht, D.J., Jahng, G.H., Liu, C.S., Rubin, J.T., Haselgrove, J., ... Detre, J.A., 2003. Pediatric perfusion imaging using pulsed arterial spin labeling. J. Magn. Reson. Imaging 18, 404–413.
Winkler, A.M., Ridgway, G.R., Webster, M.A., Smith, S.M., Nichols, T.E., 2014. Permutation inference for the general linear model. Neuroimage 92, 381–397.
Woodward, L.J., Anderson, P.J., Austin, N.C., Howard, K., Inder, T.E., 2006. Neonatal MRI to predict neurodevelopmental outcomes in preterm infants. N. Engl. J. Med. 355, 685–694.